HAL
open science

Application of Lagrangian Energy Approach to determine the Response of Isotropic Circular Plates subjected to Air and Underwater Blasts

Ye Pyae Sone Oo, Hervé Le Sourne, Olivier Dorival

To cite this version:

Ye Pyae Sone Oo, Hervé Le Sourne, Olivier Dorival. Application of Lagrangian Energy Approach to determine the Response of Isotropic Circular Plates subjected to Air and Underwater Blasts. 7th International Conference on Marine Structures - MARSTRUCT 2019, May 2019, Dubrovnik, Croatia. hal-02369105

HAL Id: hal-02369105

https://hal.science/hal-02369105v1

Submitted on 18 Nov 2019

HAL is a multi-disciplinary open access archive for the deposit and dissemination of scientific research documents, whether they are published or not. The documents may come from teaching and research institutions in France or abroad, or from public or private research centers.

L'archive ouverte pluridisciplinaire **HAL**, est destinée au dépôt et à la diffusion de documents scientifiques de niveau recherche, publiés ou non, émanant des établissements d'enseignement et de recherche français ou étrangers, des laboratoires publics ou privés.

Application of Lagrangian Energy Approach to determine the Response of Isotropic Circular Plates subjected to Air and Underwater Blasts

Y.P. Sone Oo
GeM Institute (UMR CNRS 6183) - Calcul-Meca, Nantes, France

H. Le Sourne
GeM Institute (UMR CNRS 6183) - ICAM Nantes campus, France

O. Dorival
Clément Ader Institute (FRE CNRS 3687) – ICAM Toulouse campus, France

ABSTRACT: This paper presents a simplified analytical formulation that uses Lagrangian Energy Approach to predict air and underwater blast response of air-backed simply-supported circular steel plates. Triangular and exponential pressure profiles are considered for air and underwater blast loading respectively. Calculation of the response is divided into two stages. In the first stage, maximum impulsive velocity is determined by assuming that the plate has negligible deformation and then by using the conservation of linear momentum for air blast and Taylor's one-dimensional analytical model for underwater blast. In the second stage of calculation, elastic deformation is obtained by applying the initial conditions determined from the first stage, also taking into account the rotatory inertia and water-added inertia effect. The obtained analytical solutions are tested with various plate aspect ratios as well as various loading levels and the results are compared with those from non-linear finite element explicit simulations. It is found that the proposed formulations correlate well with the finite element results giving only 5–20% discrepancy provided that the plate deflections are supposed to remain small compared to its thickness. Finally, the advantages and limitations of the present method are discussed.

1 INTRODUCTION

1.1 *State-of-the-art*

Both in-air and underwater explosions have long been a major threat for military and civil structures since World War I and II. Such loadings usually involve explosion with very high pressure, causing serious detrimental effects onto the structures. It is thus important to understand the underlying physics concerning with these loadings to promote the structural safety as well as to propose better and safer designs.

Generally, both in-air and underwater blast loading can be viewed as classical impulsive loading problem in which the initial kinetic energy is dissipated as an elastic or plastic strain energy of the structure. Indeed, a considerable body of literature already existed for this kind of problem. Mair (1999) reviewed and compiled existing analytical, empirical and numerical approaches to determine the submerged structural response of underwater explosions. Porfiri & Gupta (2009) presented a comprehensive literature review on noticeable worldwide research efforts in the field of impulsive loading submitted to the marine structures.

Theoretical studies regarding the impulsive response of steel plates or diaphragms began during the World War II. Taylor (1950), Hudson (1951) and Richardson & Kirkwood (1950) were among the first to conduct experimental and analytical studies on the dynamic plastic behavior of thin plates. Later, Hopkins & Prager (1954) studied about dynamic plastic response of simply-supported circular plate subjected to a uniformly distributed load which is brought on suddenly and then removed abruptly after a certain time interval. However, only bending deformation was considered in their analytical model and the calculation steps were given depending on the intensity of applied pressure. Symonds & Wierzbicki (1979) obtained exact theoretical membrane solution by examining the impulsively loaded circular plate behavior. Jones (1989) also proposed various analytical models for predicting infinitesimal and finite displacements of beams, plates and shells with or without taking into account the membrane action, transverse shear deformation and rotatory inertia effect. Later, this work was extended by Qiu et al. (2004) to apply for underwater shock response of monolithic and sandwich circular plates with clamped boundary condition. In this paper as well, the solutions are split into small and large displacement regime.

So far theoretical solutions from the past decades have been presented. It would however be insufficient without mentioning about the experimental tests. Florence (1966) made experimental study on large impulsive response of simply-supported circular plates and then compared with Wang (1955)'s theoretical bending solution of impulsively loaded rigid-plastic plates. It was found that disregarding the

membrane forces could seriously overestimate the final permanent deflection. A recent experimental and analytical study about the response of metallic circular plates subjected to air blast loading can be seen in Gharababaei et al. (2010). It compares the clamped plate responses using various analytical formulations available in the literature.

Coming back to the underwater explosion, Cole (1948) systematically presented about the underwater explosion and its related physical effects. Compilation of some of the earliest research works can be found through three volumes of ''Underwater Explosion Research'' issued by the office of Naval Research in 1950. Taylor (1941) proposed a one-dimensional fluid-structure interaction (FSI) model when a free-standing rigid plate with an infinite length is impacted by a plane shock wave. The finding of this paper has been proved experimentally by Deshpande et al. (2006) several decades later. Liu & Young (2008) also extended Taylor's air-backed model into water-backed FSI model. Rajendran (2001) performed experimental tests to investigate linear elastic shock response of circular and rectangular steel plates. Strain distributions across the specimen were analyzed and compared with the semi-analytical results and good agreement was achieved. A recent analytical study of cylindrical shell-shock interaction can be found in Brochard et al. (2018) which is an extension of string-on-plastic foundation model originally proposed by Hoo Fatt (1992).

According to Felippa (1980), a structure submerged in an infinite acoustic medium needs to satisfy the three-dimensional scalar wave equation and the associated FSI effect could be expressed by the exact formulation of Kirchhoff's Retarded Potential Formula (RPF). However, direct application of RPF to transient response calculations could be computationally expensive due to the need to store a vast amount of historic data when solving coupled motion equations numerically for each time step. This limitation is especially obvious when the time steps were to increase. For these reasons, approximate FSI models such as Doubly Asymptotic Approximation (DAA) model developed by Geers (1978) are applied in the field of FSI modelling. The occurrence of cavitation, see Schiffer et al. (2012), and the time evolution of water-added inertia mass also adds more complexities to the study of underwater explosion.

Nowadays, together with the advancement in computation power, it becomes possible to study the FSI problem using advanced numerical code such as Underwater Shock Analysis (USA) code. The main advantage of this method is that the governing equations are expressed in terms of wet surface variables only and thus, it is not necessary to explicitly model the surrounding fluid. Due to its robustness and relative accuracy, USA code has been incorporated with various commercial finite element codes such as LS-DYNA, NASTRAN, etc. The application of USA code in shipbuilding can be found in DeRuntz Jr. (1989) and Le Sourne et al. (2003).

1.2 *Motivation & Objectives*

Even though the application of numerical methods such as LS-DYNA/USA mentioned above seems promising, it is still prohibited in the preliminary design stages due to its complicated modelling steps and expensive computation time. In this regard, analytical solutions become very useful since they could not only provide a wide variety of design choices in a short amount of time but also give more physical insights to the problem studied.

Indeed, the objective of this paper is to propose an analytical solution when isotropic circular plates are subjected to air and underwater blasts. The plate is considered as an air-backed plate with simply-supported boundary condition at the edge. Both bending and mid-plane stretching are considered, also taking into account the rotatory inertia and water-added inertia effects. The displacements are assumed to be small compared to the plate thickness and the material stress-strain relationship obeys Hooke's law. Strain rate effect and failure are not considered in this analysis. The obtained analytical solutions are then compared with the results of non-linear finite element explicit code LS-DYNA. It is worth mentioning that the finding of this research will be utilized in the future investigation of dynamic behavior of submerged composite plates when subjected to underwater explosion with or without considering the post-damage response by making the same assumption on small displacements presented in this paper.

2 EXPLOSIVE LOADING

2.1 *Air-blast loading*

Assume that a circular steel plate having radius a, thickness h_s and density ρ_s is loaded by uniformly distributed pressure pulse which has triangular profile as follows:

$$P(t) = \begin{cases} P_0\left(1-\frac{t}{\tau}\right) & 0 \le t \le \tau \\ 0 & t \ge \tau \end{cases} \tag{1}$$

where P_0 is the peak pressure; and τ is the decay time of the shock wave.

The pressure loading in Equation 1 is used to calculate the impulse which will be transmitted to the plate as:

$$I = \int_0^\tau P_0\left(1-\frac{t}{\tau}\right)dt = \frac{1}{2}P_0\tau \tag{2}$$

Taking the conservation of linear momentum at $t = 0$ gives the following initial impulsive velocity:

$$v_i^a = \frac{P_0\tau}{2\rho_s h_s} \tag{3}$$

where the superscript 'a' is used to distinguish the air blast loading from water blast loading.

2.2 *Underwater-blast loading*

The pressure submitted to the plate due to underwater explosion can be considered as near-field or far-field depending on the stand-off distance. The treatment on the compressibility of water and other important physical parameters can vary for near-field and far-field explosions. For the present analysis, it is assumed that the plate is sufficiently far enough from the explosive charge so that a plane shock assumption can be considered. Then, the pressure loading which acts on the target can be split into two phases. In phase I, early-time approximation is considered and the impulsive velocity is derived based on the procedures given in Cole (1948) and Taylor (1941). In phase II, long-time approximation is considered. Simplified RPF expression for circular plate is applied, assuming that there is no more incident pressure and the water-added inertia arises during plate deceleration.

2.2.1 *Pressure loading in Phase I*

Now suppose that a circular steel plate with radius a, thickness h_s and density ρ_s is in contact with water of density ρ_w on one side and air on the other side. It is then loaded by a planar exponentially decaying pressure pulse having a peak pressure P_0, decay time τ and traveling at sonic speed c_w in water towards the plate as shown in Figure 1. The one-dimensional incident pressure wave P_i at any arbitrary time t and at any distance z from the fluid-structure boundary OO' can be written as:

$$P_i(t) = P_0 e^{(-t/\tau\ +\ z/c_w)} \quad 0 \le t \le \tau \tag{4}$$

Note that polar coordinate (r, θ and z) system is used. The origin of the coordinate is taken at the boundary OO' and at the centre of the plate. The z-axis is positive for downward direction which is also the same direction for the incident wave.

The peak pressure P_0 and decay time τ involved in Equation 4 can be determined by using the principle of similarity. The principle of similarity states that the pressure and other properties of the shock wave will be the same if the scales of length and time are varied by the same scale factor. Using this principle and the property of TNT explosive, the peak pressure and decay constant can be given as a function of explosive mass W in kg and stand-off distance R in m as:

$$P_0 = 52.117 \times 10^6 \left(\frac{W^{1/3}}{R}\right)^{1.18} \ (Nm^{-2}) \tag{5}$$

$$\tau = 0.09 \times W^{1/3} \left(\frac{W^{1/3}}{R}\right)^{-0.185} \ (ms) \tag{6}$$

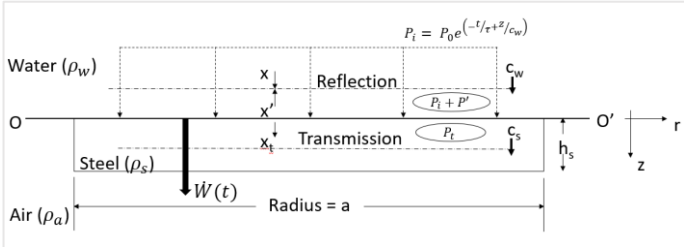

Figure 1. Pressure and particle velocity fields at the boundary

As shown in Figure 1, the problem is treated as a 1D problem in which only the transverse displacements are considered. Henceforth, the tangential components of the velocity for both particles and the plate are assumed to vanish. The particle velocities for incident, reflected and transmitted wave in the transverse direction are denoted as x, x' and x_t respectively and the plate velocity as $\dot{W}$. Note that the plate in this case is assumed to behave like a free-standing plate with negligible amount of deformation until it reaches the maximum impulsive velocity v_i^w.

Upon arrival of the pressure wave at OO', part of the incident pressure is reflected back into the fluid while the other part is transmitted into the plate depending on the mechanical impedance of the plate's material. For steel, the mechanical impedance can be expressed as:

$$Z_s = \rho_s c_s \tag{7}$$

where $c_s = \sqrt{\frac{E(1-\nu)}{\rho(1+\nu)(1-2\nu)}}$ is the sonic speed in steel.

Let us say the incident pressure at the interface ($z = 0$) is:

$$P_i = P_0 e^{-t/\tau} \tag{8}$$

The reflected pressure can be described as:

$$P' = P_0 \varphi(t) \tag{9}$$

where $\varphi(t)$ is a temporal function to be determined. Note that $\varphi(t)$ will decay with time and is actually a component of the reflection and radiated waves due to the transverse movement of the plate $\dot{W}(t)$.

The transmitted pressure can be written as a function of incident pressure according to Cole (1948):

$$P_t = \frac{2\rho_s c_s}{\rho_s c_s + \rho_w c_w} P_i \tag{10}$$

By taking the velocity continuity at the fluid-structure interface OO' and by assuming pressure and particle velocities for sufficiently small disturbances as has been done by Cole (1948), the following equation for φ can be derived:

$$\varphi = \frac{1}{P_0}\left(\mu P_0 e^{-t/\tau} - \rho_w c_w \dot{W}\right) \tag{11}$$

where $\mu = \frac{\rho_s c_s - \rho_w c_w}{\rho_s c_s + \rho_w c_w}$ is the reflection parameter. In the case of rigid boundary, $\rho_w c_w \ll \rho_s c_s$ so that the reflection parameter $\mu \approx 1$.

By substituting Equation 11 in Equation 9 and then using Equation 8, the total pressure for phase I can be expressed as:

$$P(t)^I = (1+\mu)P_0 e^{-t/\tau} - \rho_w c_w \dot{W} \quad (12)$$

Now by considering the plate initial kinetic energy and the external pressure loading from Equation 12, the following equation of motion can be obtained:

$$\rho_s h_s \ddot{W} + \rho_w c_w \dot{W} = (1+\mu)P_0 e^{-t/\tau} \quad (13)$$

The solution of Equation 13 has already been given by Taylor (1941) and the plate will reach the maximum impulsive velocity:

$$v_i^w = \frac{(1+\mu)\xi P_0 \tau}{\rho_s h_s} \quad (14)$$

at corresponding cavitation inception time as:

$$t_c^w = \frac{\tau \, ln\psi}{\psi - 1} \quad (15)$$

where $\xi = \psi^{-\frac{\psi}{\psi-1}}$; and $\psi = \frac{\rho_w c_w \tau}{\rho_s h_s}$. Here again, the superscript letter 'w' is introduced to differentiate the water-blast parameters from the air-blast ones.

2.2.2 *Pressure loading in Phase II*

As discussed above, the deformation of the plate is supposed to commence in the second phase of the response. By assuming that the incident pressure field vanishes and the associated plate deceleration produces the water-added inertia mass, the approximate form of Kirchhoff RPF for circular plate will take the following:

$$P(t)^{II} \approx -\frac{\rho_w}{2\pi}\int_0^{2\pi}\int_0^a \frac{\partial \dot{w}}{\partial t} dr d\theta \quad (16)$$

In applying Equation 16 to the assumed deformed shape, it should be aware that the added mass will evolve over time starting from t_c^w until the plate reaches the maximum deformation. The additional impulse caused by the added mass pressure is given as:

$$I_{add} = \int_{t_c^w}^{T_{max}} P(t)^{II} dt \quad (17)$$

where T_{max} = the time required for the plate to reach maximum deformation.

Considering this effect in the derivation makes the equations non-linear and thus, equivalent parameter C^* is introduced in this paper. By assuming $t_c^w \ll 1$, the equivalent parameter C^* can be expressed as a linear function of the ratio h/a of the circular plate as:

$$C^* = \frac{I_{add}}{P(t)^{II} T_{max}} \approx K_a \frac{h}{a} \quad (18)$$

where K_a = approximation factor for added mass for $0 \le K_a \le a/h$. The constant K_a also depends on the type of plate geometry. In this paper, K_a is taken as 9 which is obtained by fitting the numerical results using various *h/a* ratios of circular plates and various applied impulses. Nevertheless, it is clear that this approximation factor is valid only for circular plates and such method to account for water inertia effects needs to be improved in the future.

3 ANALYTICAL FORMULATION

3.1 *Problem formulation*

The same circular plate from the previous section is considered. To calculate the plate deformation, assume that the plate's transverse displacement is separable into temporal and spatial variables as:

$$w(r,t) = W(t)\left(1 - \frac{r^2}{a^2}\right) \quad 0 \le r \le a \quad (19)$$

where $W(t)$ is the maximum deflection at the plate center; r the radial coordinates; and a the radius of the plate. Note that the above equation is in consistence with the hypothesis of the parabolic axisymmetric deformation profile of circular plates under impulsive loads. Equation 19 also satisfies simply-supported boundary condition requirement at $r = a$ and $r = 0$.

Moreover, the following assumptions are further imposed.

- In-plane displacements are negligible compared to the transverse displacement:
  $$|u|, |v| \ll |w|$$
- The problem is axisymmetric (no θ term is considered in Eq. 19)
- The loading is uniform pressure pulse distributed all over the plate or impulsive velocity
- Radial and circumferential strains are the only significant terms while:
  $$\varepsilon_{zz} \approx \varepsilon_{rz} \approx \varepsilon_{\theta z} \approx \varepsilon_{r\theta} \approx 0$$
- Mid-plain strain is derived by using Cauchy strain expression for circular plate and then by expanding into Taylor series and keeping only the first two terms as:
  $$\varepsilon_r = \sqrt{1 + \left(\frac{\partial w}{\partial r}\right)^2} - 1 \approx \frac{1}{2}\left(\frac{\partial w}{\partial r}\right)^2 \quad (20)$$
- The curvature has the following relationship:
  $$\kappa_r = -\frac{\partial^2 w}{\partial r^2} \quad \kappa_\theta = -\frac{1}{r}\frac{\partial w}{\partial r} \quad (21)$$
- The plate is assumed to be made with isotropic materials. Then, the flexural rigidity D can be given as:
  $$D = \frac{Eh^3}{12(1-\nu^2)} \quad (22)$$
  where E and ν are Young modulus and Poisson's ratio of the material respectively.
- The stress-strain relations obey Hooke's law:
  $$\begin{bmatrix}\sigma_r \\ \sigma_\theta\end{bmatrix} = \frac{E}{1-\nu^2}\begin{bmatrix}1 & \nu \\ \nu & 1\end{bmatrix}\begin{bmatrix}\varepsilon_r + z\kappa_r \\ z\kappa_\theta\end{bmatrix} \quad (23)$$

The above assumptions lead to the following strain energy for mid-plane radial stretching as:

$$U_s = \frac{1}{2}\int_{-h/2}^{h/2}\int_0^{2\pi}\int_0^a \left[\sigma_r \frac{1}{2}\left(\frac{\partial w}{\partial r}\right)^2\right] r dr d\theta dz \quad (24)$$

and the general bending strain energy as follows:

$$U_b = \int_0^{2\pi}\int_0^a \frac{D}{2}\left[\left(\frac{\partial^2 w}{\partial r^2} + \frac{1}{r}\frac{\partial w}{\partial r}\right)^2 - 2(1-\nu)\frac{\partial^2 w}{\partial r^2}\left(\frac{1}{r}\frac{\partial w}{\partial r}\right)\right] r dr d\theta \quad (25)$$

Using Equations 19-25 will yield the following non-linear strain energy expression in which the first term corresponds to stretching strain energy and the second term corresponds to bending strain energy:

$$U = \frac{2\pi hE}{3(1-\nu^2)}\left(\frac{W^2}{a}\right)^2 + 4\pi D(1+\nu)\left(\frac{W}{a}\right)^2 \quad (26)$$

Similarly, the kinetic energy T is also derived using the following general expression:

$$T = \frac{1}{2}\int_0^{2\pi}\int_0^a\int_{-h/2}^{h/2}\rho(\dot{u}^2+\dot{v}^2+\dot{w}^2)\,dzrdrd\theta \quad (27)$$

Solving Equation 27 will give the following equation:

$$T = \left[\frac{\pi\rho h^3}{12} + \frac{\pi a^2\rho h}{6}\right]\dot{W}^2 \quad (28)$$

Finally, Equations 27 and 28 are solved in general Lagrangian Equation:

$$\frac{d}{dt}\left(\frac{\partial L}{\partial \dot{q}}\right) - \left(\frac{\partial L}{\partial q}\right) = Q \quad (29)$$

where $L = T - U$; q is the generalized coordinate; and Q the non-conservative force due to external load. In the present case, the generalized coordinate is the central deflection $W(t)$ and its velocity $\dot{W}(t)$.

Solving of Equations 26-29 gives the following general expression of equation of motion:

$$A_1\ddot{W}(t) + A_2W(t)^3 + A_3W(t) = 0 \quad (30)$$

where A_1, A_2 and A_3 are constants that depend on the blast loading type and will be determined in the following sub-sections.

3.2 *Air-blast response*

Air-blast problem is treated as initial value problem by giving the initial condition of W and $\dot{W}$ at $t = 0$. The initial condition for plate velocity $\dot{W}$ can be derived by equating the initial kinetic energy into Equation 28. At $t = 0$,

$$T = \frac{1}{2}\rho h\pi a^2 {v_i}^2 = \left[\frac{\pi\rho h^3}{12} + \frac{\pi a^2\rho h}{6}\right]\dot{W}(0)^2 \quad (31)$$

By solving Equation 31, the initial condition for plate velocity $\dot{W}(0)$ is obtained. Now the initial conditions are:

$$W(0) = 0 \qquad \dot{W}(0) = \sqrt{3}v_i \quad (32)$$

where v_i should be determined from Equation 3. The constants A_1, A_2 and A_3 are determined as:

$$A_1 = \frac{\pi\rho h^3}{6} + \frac{\pi a^2\rho h}{3}$$
$$A_2 = \frac{8\pi hE}{3a^2(1-\nu^2)} \quad (33)$$
$$A_3 = \frac{8\pi D(1+\nu)}{a^2}$$

Note that the first term of A_1 refers to rotatory inertia effect and the second term the mass inertia effect; A_2 denotes the non-linear membrane stiffness; and A_3 represents the bending stiffness.

Now substituting Equation 33 into Equation 30 and using Equation 32 as initial condition, the resulting equation of motion can be solved numerically.

3.3 *Underwater-blast response*

Underwater blast response has the same form of equation of motion (Eq. 30), however, water-added mass must be taken into account. As already explained in section 2.2.2, the additional pressure caused by water-added inertia will be determined by using Equation 16. Taking into account the equivalent parameter C^* to approximate the temporal evolution of water-added mass, the pressure loading in Phase II can be given as:

$$P(t)^{II} \approx -\frac{2}{3}C^*\rho_w a\ddot{W} \quad (34)$$

Equation 34 can be used to derive external non-conservative force term Q from Equation 29 as:

$$Q = \int_0^{2\pi}\int_0^a\left[-\frac{2}{3}C^*\rho_w a\ddot{W}\right]rdrd\theta \quad (35)$$

Taking into account Equation 35 in Equation 30 and applying Equation 32 as an initial condition, the constants A_1, A_2 and A_3 can be derived. The constants A_2 and A_3 are the same as described in Equation 33 while the constant term A_1 becomes:

$$A_1 = \frac{\pi\rho h^3}{6} + \frac{\pi a^2\rho h}{3} + \frac{2}{3}C^*\rho_w\pi a^3 \quad (36)$$

Again, the resulting equation of motion can be solved numerically. Note that the initial velocity v_i in Equation 32 should use v_i^w from Equation 14 for underwater blast.

4 NUMERICAL ANALYSIS

Numerical simulations are performed by using the non-linear finite element explicit code LS-DYNA. Detailed modelling steps will be given depending on the type of loading in the next sections. The material properties are given in Table 1 in which three *h/a* ratios are considered, keeping the same areal mass, i.e., the same thickness for each *h/a* ratios.

Table 1. Characteristics of the material

h/a	0.1	0.06*	0.02
Radius *a* (m)	0.0612	0.1016	0.3061
Thickness h_s (m)	0.0061	0.0061	0.0061
Density ρ_s (kgm^{-3})	7822.8	7822.8	7822.8
Young modulus *E* (Nm^{-2})	2.07×10^{11}	2.07×10^{11}	2.07×10^{11}
Poisson ratio υ	0.3	0.3	0.3
Yield stress σ_y (Nm^{-2})	5.45×10^{8}	5.45×10^{8}	5.45×10^{8}

* Taken from the paper of Florence (1966)

4.1 *Air-blast response*

For air-blast loading, the pressure boundary condition is prescribed directly onto the 2D finite element plate. A typical finite element model for $h/a = 0.06$ is shown in Figure 2. The mesh adapted for different *h/a* ratios of the circular plate is between 3 – 7 mm. This mesh size has been ensured to be sufficiently fine enough to capture the correct deformation amplitude as well as the participating mode shapes. The peak pressure used are only between 1 – 10 MPa to make sure that the plate deformations remain small compared to the plate thickness and the material response is still within the elastic limit. The decay time of 0.05ms is applied for all pressure loading levels. The plate is modeled using **MAT_PIECEWISE_LINEAR_PLASTICITY* LS-DYNA card based on the properties given in Table 1 without considering the strain rate effect. Shell elements with Belytschko-Tsay formulation are used. Five integration points are considered throughout the thickness. Simply-supported boundary condition is achieved by restraining the displacements at the edges but allowing for the rotations.

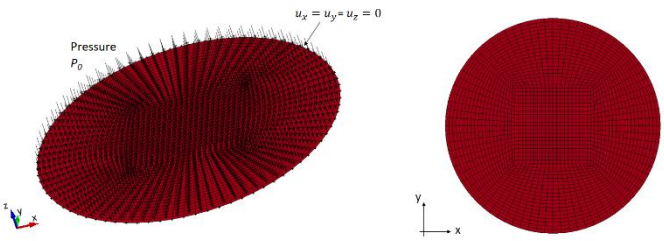

(a) Pressure and boundary conditions (b) Mesh size

Figure 2. Typical finite element model for air-blast simulation

4.2 *Underwater-blast response*

The FE model for the underwater-blast contains two parts: the fluid part and the structure part. The former is modeled using material ACOUSTIC with acoustic solid element formulation (ELFORM 8) in LS-DYNA. The latter is modeled using *MAT _PIECEWISE_LINEAR_PLASTICITY with Belytschko-Lin-Tsay shell element formulation. Strain rate and hydrostatic pressure effects are ignored in the analysis too.

The length of the fluid column is considered 0.25 m. The mesh size of the fluid element is 1 mm in the thickness direction (negative z-direction). The fluid mesh in the x-y plane is used the same as the circular plate mesh in the x-y plane. The mesh size of the circular plate for the underwater-blast is the same as the mesh size used in the air-blast loading model of the plate, i.e., between 3 – 7 mm for the corresponding *h/a* ratio. Note that the selection of the mesh size and the fluid column length have been confirmed by running a number of simulations using only one column of fluid and structural elements. It was found that since only 1D plane shock wave is considered, the aspect ratio of the fluid element has no effect on the solutions. Also, the choice of the fluid column length ensures that no returning waves from the boundary influences the plate deformation process. The nodes of the structure and fluid are merged together so that the fluid-structure coupling is automatically treated in LS-DYNA. The lateral surface of the fluid elements is constrained in x and y directions to make sure that 1D wave propagation is properly simulated. The pressure loading that ranges from 1 – 10 MPa with 0.081 ms decay time is prescribed as a load boundary at one end of the fluid model and at the other end, the circular plate model is attached by using simply-supported boundary conditions (see Fig. 3). Cavitation is considered in the analysis by defining the pressure cut-off so that when the pressure becomes negative, it will be forced to zero. Numerical damping (BETA = 0.25) is applied on the acoustic fluid element. The consequence of this is having a slightly less peak pressure value at the plate. However, analyzing the pressure results and impulse at the nearest element to the plate shows that the results are in accordance with the transferred impulse value provided by Taylor's FSI formulation at the early-time response. To study the influence of FSI effect, numerical simulations are also performed by using only the impulsive velocity given by Taylor's FSI model (Eq. 14).

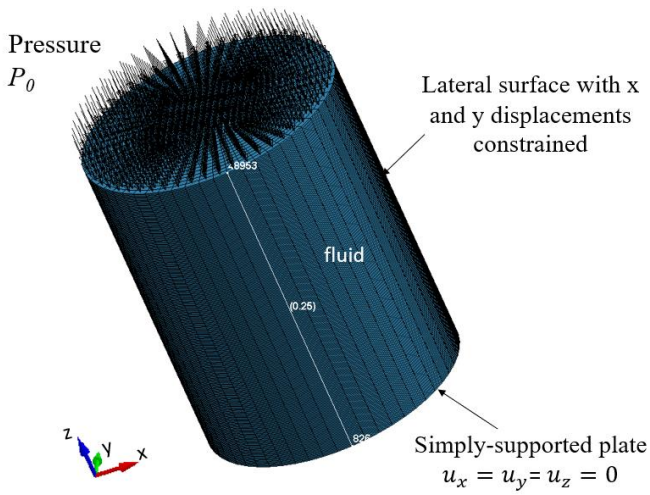

Figure 3. Typical finite element model for underwater-blast simulation

5 RESULTS & DISCUSSION

5.1 *Air-blast response*

The central deflection-time history for the air-blast loading with *h/a* ratio of 0.1 and peak pressure 5 MPa is shown in Figure 4. It can be seen that analytical solution predicts quite well the maximum deformation with 10% discrepancy. However, it is observed that the FEA solutions contain higher order vibration modes and the final result is the combination of all modal shapes whereas the analytical solution only gives the result of first order mode shape. This leads to the analytical results to have a different peak

response time (about 30% discrepancy) as compared with LS-DYNA. Another limitation of the current model is the assumption on the transverse deformed profile which is supposed to have the same deformation mode shape for every time step. This is not true in reality since there is a propagation of a shear wave that starts from the boundary and travels towards the plate center and then the deformation continues. The current model simply ignores this wave propagation step for simplicity of the solution, knowing that the initial velocity field will not have exactly the same mode shape assumed in this paper. This may cause the kinetic energy transmitted to the plate to be slightly different than what has been predicted in the analytical model.

The central deflection-thickness ratio of the plate is compared against different levels of dimensionless impulses ϕ in Figures 5 – 7 for different *h/a* ratios. In general, it can be said that the discrepancy increases as the *h/a* ratio decreases. For each *h/a* ratio, the analytical results underestimate about 10–20% less central-deflection compared to LS-DYNA. However, the response of *h/a* = 0.02 are in fact no longer small displacement solutions and clearly the response is no longer linear due to the occurrence of slight yielding and to the fact that membrane mode deformation becomes predominant.

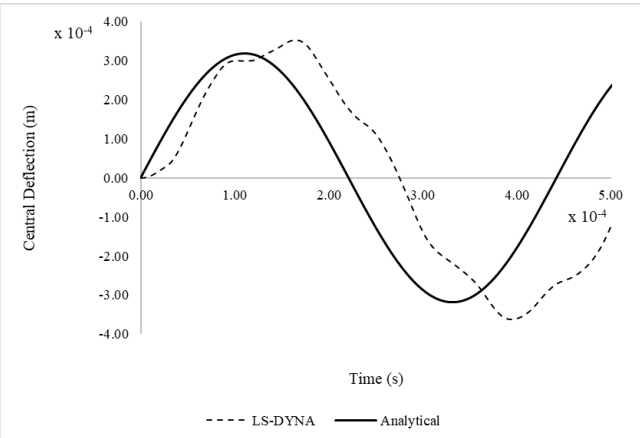

Figure 4. Central deflection-time history for air-blast (h/a = 0.1, P_0 = 5 MPa, τ = 0.05 ms)

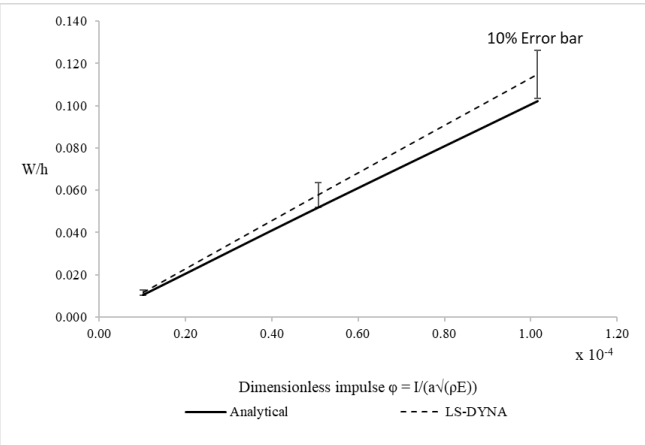

Figure 5. Plots of central deflection-thickness ratio for different impulses of air-blast loading (h/a = 0.1)

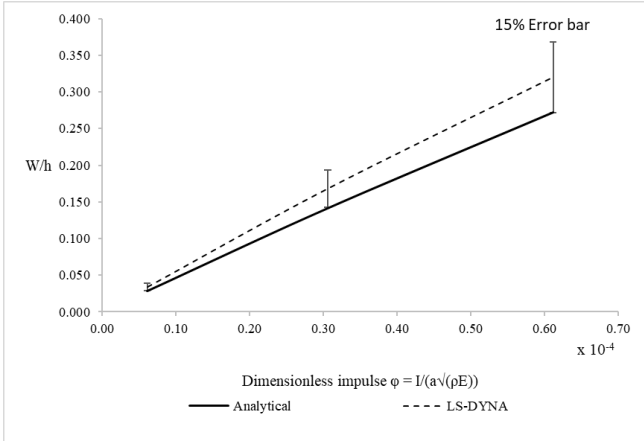

Figure 6. Plots of central deflection-thickness ratio for different impulses of air-blast loading (h/a = 0.06)

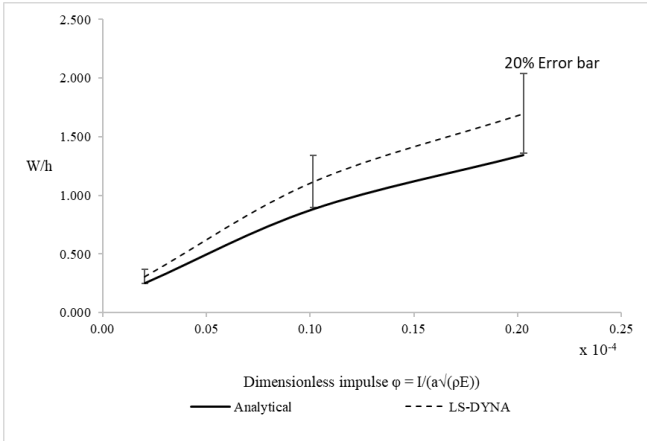

Figure 7. Plots of central deflection-thickness ratio for different impulses of air-blast loading (h/a = 0.02)

5.2 *Underwater-blast response*

The central deflection-time history for underwater-blast loading using a peak pressure of 10 MPa is shown in Figure 8. It can be seen that the current analytical result predicts well in terms of the peak response amplitude as well as the peak response time. However, the influence of higher order vibration modes and the modal sum results could be clearly seen in the FEA/LS-DYNA results.

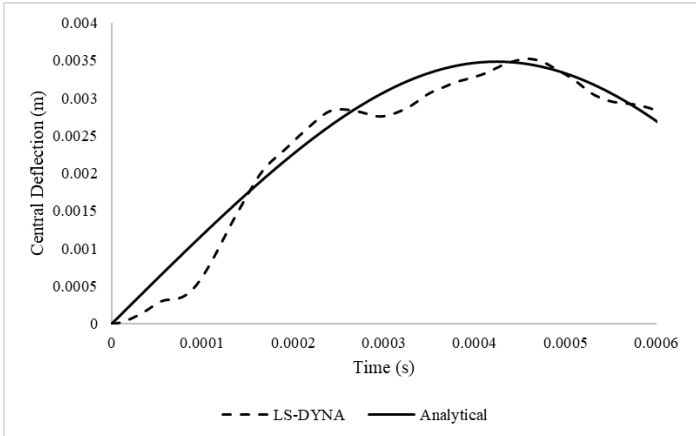

Figure 8. Central deflection-time history for underwater-blast (h/a = 0.06, P_0 = 10 MPa, τ = 0.081 ms)

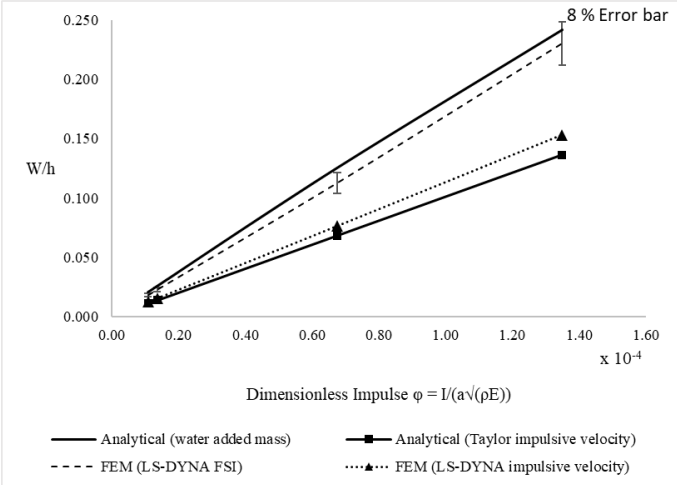

Figure 9. Plots of central deflection-thickness ratio for different impulses of underwater-blast loading (*h/a* = 0.1)

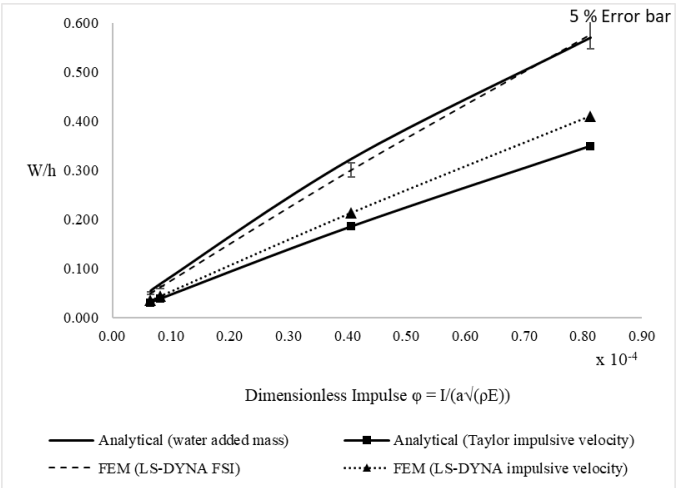

Figure 10. Plots of central deflection-thickness ratio for different impulses of underwater-blast loading (*h/a* = 0.06)

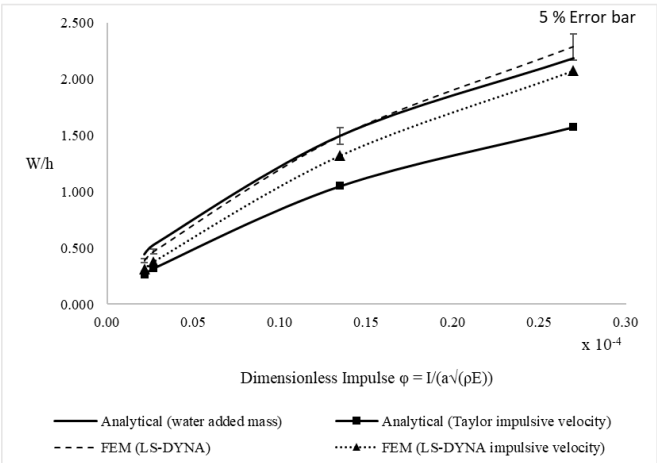

Figure 11. Plots of central deflection-thickness ratio for different impulses of underwater-blast loading (*h/a* = 0.02)

The plots of central deflection-thickness ratio for different levels of dimensionless impulses ϕ are shown in Figures 9 – 11, each representing a different *h/a* ratio. In order to highlight the significance of water-added mass in the second phase of the loading, the analytical results with or without considering the water-added mass effect, i.e., the constant A_1 with or without the water-added inertia term $2/3\ C^*\rho_w\pi a^3$. For better comparison, the finite element results using only the Taylor's impulsive velocity without explicitly modelling the fluid model are also included. Note that all of the model compared have the same areal mass by keeping the same thickness and mass density. It can be observed that the current analytical model correlates well with the finite element results with FSI effect, only showing a discrepancy range of 5–8%. It can be found that the results without considering water-added mass effect could lead to significant underestimation of the response especially for high *h/a* ratio. The results of finite element model and the analytical one show a similar trend with air-blast model when the water-added mass effects are disregarded. Here, it should be noticed that the proposed equivalent correction factor C^* compensates well the time-evolution of the water-added mass function.

6 CONCLUSION & FUTURE WORKS

In this paper, a simplified analytical model is proposed using Lagrangian Energy Approach to derive the equation of motions when the air-backed simply-supported isotropic circular plates are subjected to air-blast and underwater-blast loadings. The calculation steps are divided into two stages. In stage I, the plate is assumed to have negligible amount of deformation and then the initial impulsive velocities are derived depending on the type of loading. For air-blast loading, the corresponding impulsive velocity is derived by using the conservation of linear momentum whereas for underwater-blast, it is obtained based on Taylor's 1D FSI model. Then, in stage II, the plate deformation is supposed to commence and the water-added mass inertia increases overtime due to plate deceleration and collapse of the cavitation zone. The impulsive velocity determined from the first stage is used as an initial condition for the second stage. The cavitation near the structure is supposed to occur at the end of the first stage and water inertia forces appear in the second stage. To compensate the time-lapse between the two stages, an equivalent parameter C^* is introduced depending on the plate *h/a* ratio. Both air-blast and underwater-blast responses are given for various aspect ratios as well as various impulses. The same calculations are performed using non-linear finite element software LS-DYNA. Comparison of the results from both approaches shows that there is a discrepancy of 10-20% for air-blast and 5-8% for underwater-blast. For an analytical formulation, this seems a pretty promising approach.

Of course, there are a few drawbacks too. For example, the higher order vibration modes are not considered in the present model. In fact, the results shown by FEM is the sum of all modal participation of different mode shapes. Another limitation is that the deformation profile is supposed to remain constant for

all time steps which is not true in reality. There is a propagation of flexural wave front that emanates from the plate boundary and then travels towards the center of the plate. The bending and shear deformations are developed behind its front and thus, this effect must be taken into account in order to accurately model the correct deformed shape for all time histories. Also, for underwater-blast, the equivalent parameter C^* is given as a function of the plate *h/a* ratio using the coefficient K_a to compensate for an abrupt transition from the first to the second stage. However, no rigorous justifications have been given regarding the emergence of the coefficient K_a nor C^*. Moreover, the effect of hydrostatics pressure, strain rate and geometrical change as well as large deformation effects are ignored in the present analytical approach.

In the future, the approach will be extended to couple with Doubly Asymptotic Approximation model of Geers (1978) for better modelling of pressure loading. The extension of the present approach for different geometries, a square plate for instance, will be carried out. Then, finally, it is the objective of the authors to apply the same approach on submerged marine composite plates to investigate their dynamic responses with or without considering the post-damaged behavior.

7 ACKNOWLEDGMENT

This research work has been conducted with the financial support of DGA-DGE. The authors would also like to thank Calcul-Meca and Multiplast companies for their technical support.

8 REFERENCES

Brochard, K., Le Sourne, H., and Barras, G. 2018. Extension of the string-on-foundation method to study the shockwave response of an immersed cylinder. *International Journal of Impact Engineering*, 117(May 2017):138–152.

Cole, R. H. 1948. *Underwater explosions*. Princeton University Press, Princeton.

DeRuntz Jr., J. A. (1989). The underwater shock analysis code and its applications. In *Proceedings of the 60th Shock and Vibration Symposium* (pp. 89–107).

Deshpande, V., Heaver, A., and Fleck, N. 2006. An underwater shock simulator. In *Proceedings of the Royal Society A*, number 462, pages 1021–1041, Cambridge, UK.

Felippa, C. A. 1980. A family of early-time approximations for fluid-structure interaction. *Journal of Applied Mechanics*, *47*, 703–708.

Florence, A. L. 1966. Circular plate under a uniformly distributed impulse. *International Journal of Solids and Structures*, *2*(601), 37–47.

Geers, T. L. 1978. Doubly asymptotic approximations for transient motions of submerged structures. *The Journal of the Acoustical Society of America*, 64:1500–1508.

Gharababaei, H., Darvizeh, A., & Darvizeh, M. 2010. Analytical and experimental studies for deformation of circular plates subjected to blast loading. *Journal of Mechanical Science and Technology*, *24*(9), 1855–1864.

Hoo Fatt, M. S. 1992. *Deformation and rupture of cylindrical shels under dynamic loading*. Massachusetts Institute of Technology.

Hopkins, H. G., & Prager, W. (1954). On the dynamics of plastic circular plates. *Journal of Applied Mathematics and Physics*, *5*, 317–330.

Hudson, G.E., 1951. A theory of the dynamic plastic deformation of a thin diaphragm. *Journal of Applied Physics*. Vol. 22, No. 1.

Jones, N., 1989. *Structural Impact*. Cambridge University Press, Cambridge, UK.

Le Sourne, H., County, N., Besnier, F., Kammerer, C., & Legavre, H. (2003). LS-DYNA Applications in Shipbuilding. *4th European LS-DYNA Users Conference*, 1–16.

Liu, Z. and Young, Y. L. 2008. Transient response of submerged plates subject to underwater shock loading: An Analytical Perspective. *Journal of Applied Mechanics - Transactions of the ASME 75*.

Mair, H. U. 1999. Benchmarks for submerged structure response to underwater explosions. *Shock and Vibration*, 6(4):169–181.

Office of Naval Research 1950. *Underwater Explosion Research: a compendium of British and American reports*, Vol. I, II, III. Dept. of the Navy, Washington, D.C.

Porfiri, M. and Gupta, N. 2009. A review of research on impulsive loading of marine composites. *Major Accomplishments in Composite Materials and Sandwich Structures*: An Anthology of ONR Sponsored Research: 169–194.

Qiu, X., Deshpande, V. S., & Fleck, N. A. 2004. Dynamic response of a clamped circular sandwich plate subject to shock loading. *Journal of Applied Mechanics*, *71*(September), 637–645. https://doi.org/10.1115/1.1778416.

Rajendran, R., & Narasimhan, K. 2001. Linear elastic shock response of plane plates subjected to underwater explosion. *International Journal of Impact Engineering*, 493–506.

Richardson, J.M., and Kirkwood, J.G., 1950. Theory of the plastic deformation of thin plates by underwater explosions. *Underwater Explosion Research, Vol. III, The Damage Process*: 107-121, Office of Naval Research, Dept. of the Navy, Washington, D.C.

Schiffer, A., Tagarielli, V., Petrinic, N., and Cocks, A. 2012. The response of rigid plates to deepwater blast: analytical models and finite element predictions. *Journal of Applied Mechanics*, 79.

Symonds, P.S., and Wierzbicki, T. 1979. Membrane mode solutions for impulsively loaded circular plates. *Journal of Applied Mechanics*, 46(1), 58-64.

Taylor, G. 1941. The pressure and impulse of submarine explosion waves on plates. In *The Scientific Papers of G. I. Taylor, Vol. III*, pages 287–303. Cambridge University Press, Cambridge, UK.

Taylor, G. I., 1950. The distortion under pressure of a diaphragm which is clamped along its edge and stressed beyond the elastic limit. *Underwater Explosion Research, Vol. III, The Damage Process*: 107-121, Office of Naval Research, Dept. of the Navy, Washington, D.C.

Wang, A. 1955. The permanent deflection of a plastic plate under blast loading. *Journal of Applied Mechanics*, *22*, 375–376.